Proceedings in Manufacturing Systems, Volume 10, Issue 2, 2015, 77–82 ISSN 2067-9238

EFFECTS OF LASER CLADDING PARAMETERS ON MICROSTRUCTURE PROPERTIES AND SURFACE ROUGHNESS OF GRADED MATERIAL

Franc CUS[1,*], Uros ZUPERL[2], Tomaz IRGOLIC[3]

[1)] Prof., PhD, Head of Production Engineering Institute, Faculty of Mechanical Engineering, University of Maribor, Maribor, Slovenia
[2)] Assist. Prof., PhD, Production Engineering Institute, Faculty of Mechanical Engineering, University of Maribor, Maribor, Slovenia
[3)] Assist. Production Engineering Institute, Faculty of Mechanical Engineering, University of Maribor, Maribor, Slovenia

Abstract: *This paper shows the general properties of laser cladding that have recently added new possibilities for the local surface repairing of metal mechanical elements. Despite the fact that the technology for laser cladding is highly developed any obtained surface roughness cannot not be predicted and usually additional grinding or milling process are needed to obtain the required surface roughness. Bad surface roughness is undesirable and additional machining is needed for improving surface quality. Milling was chosen in order to improve roughness. The basic idea of the research was to measure the cutting forces under different cutting conditions and produce a model that would be able to predict cutting forces by milling layers of functionally graded material at different cutting parameters. The first basic prediction model was obtained by measuring the cutting forces in the three main directions of the coordinate system by milling clad layer and changing the cutting parameters.*

Key words: *milling, functionally-graded material, laser cladding, artificial neural network.*

1. INTRODUCTION

Laser cladding of metallic materials (powders) has recently allowed us to repair damaged tool parts and also manufacture complex machine parts. The only problem of machines for laser cladding is their repeatability, optimal choices of operating parameters, and re-machining of the cladded surface which is quite rough and often unacceptable for the final product. Capello et al. [1] and Brandt et al. [4] presented the usefulness of laser cladding on real problems throughout industry. They repaired broken turbine blades and had the same problems with the repeatability of laser cladding machines as we have.

After reviewing significant literature, it was discovered that to date no one has dealt with the surface roughness and re-machining (grinding or milling) arena after laser cladding. So far model for prediction of final surface roughness of workpiece after laser cladding hasn't been developed jet. That is why we at the Faculty of Mechanical Engineering in Maribor started doing research into finding any connections between the optimal parameters of the machine for laser cladding, the resulting surface roughness according to specific machine parameters (laser power, the amount of metal powder) and the cutting forces regarding the milling process (re-machining).

The process is often used to radically improve the overall mechanical properties, increase corrosion resistance and repair worn parts and engravings [3, 4] or for producing metal composites [5]. During the process of laser cladding, commercially known as LENS (Eng. Laser Engineered Net Shaping) lasers with high power (500 W to 4 kW) are used.

2. LASER CLADDING

Laser cladding [1, 2] is the process of accumulating material in the form of powder or in the form of a wire to the base material by using a laser. The purpose of such manufacturing technologies is to coat a particular part of the base material (substrate) or create a shape close to the final form (repair of the engraving regarding the tool).

The working parameters of the Optomec LENS 850R laser-cladding machine used for our experiments are shown in Table 1.

Lasers are used to melt metal powders and combine them within a three-dimensional structure. The powder used during the laser cladding is usually metallic and is injected through a nozzle. The interaction between the added metal powder, basic material and laser beam is called the "melting zone". Examples of clad layers loaded on the base materials are shown in Figs. 1, 2 and 3.

Molten added metal then adheres to the base material, the movement of the base material allows the melt to cool down, and thereby a part or track of welded metal arises.

Table 1

Characteristics of Optomec LENS 850R

Characteristics	Value	Unit
Working area	900 x 1500 x 900	mm
Nozzle movement speed	60	mm/s
Max. deposit of material	500	g/h
Max. laser power	1000	W

[*] Corresponding author: University of Maribor, Faculty of Mechanical engineering, Smetanova 17, 2000 Maribor, Slovenia
Tel.: 00386 2 220 76 20
Fax: 00386 2 220 79 96
E-mail addresses: *franc.cus@um.si*

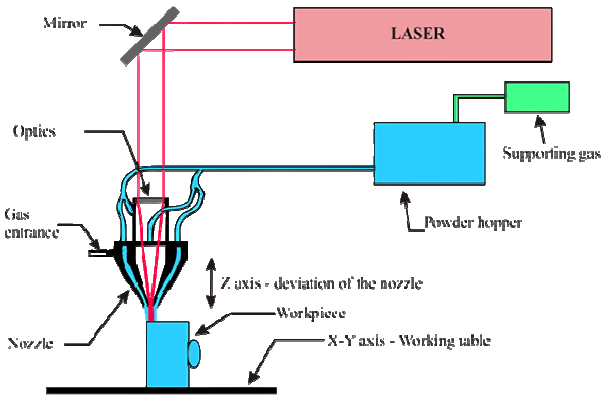

Fig. 1. Principle of laser cladding.

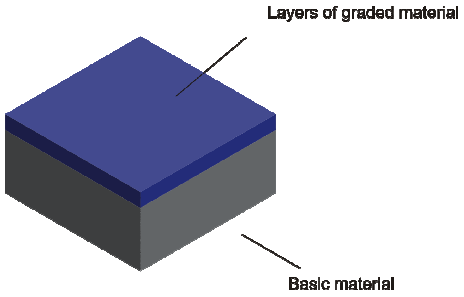

Fig. 2. A sample of laser cladding layers.

Fig. 3. Real workpiece with different cladded material zones.

The aim of the research was to build a database that would store all the optimal parameters of the final product and which would give us predicted data on the basis of forecasts by using the artificial methods for every repair with laser cladding of the new piece using the totally new geometry (as shown in Fig. 4).

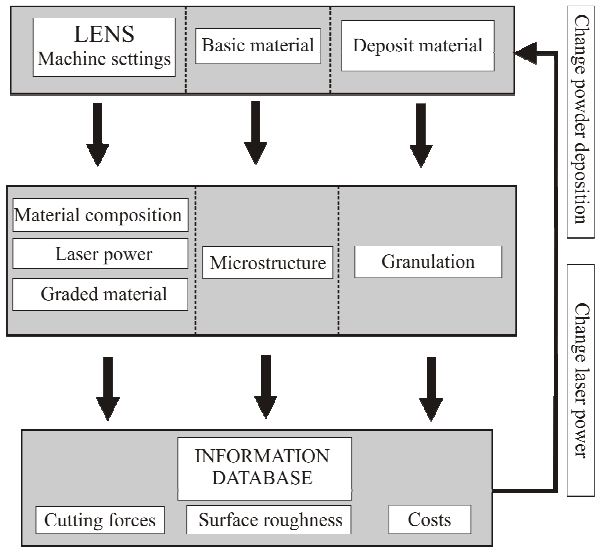

Fig. 4. Simplified model linking the laser cladding machine and reaching with milling process.

This database would help us by choosing a proper filler material, by setting optimal laser-cladding parameters and, of course, the resulting surface roughness after the laser-cladding process. Very good surface quality, which would not require a lot of re-machining (grinding and milling), could be achieved by considering all those recommendations achieved in the previous samples.

3. OPTICAL SCANNING

Information about objects within surrounding spaces and areas could be obtained using a variety of measurements. One of the newer techniques is 3D laser scanning. As it has an obvious advantage over other methods in the comprehensive capture of spatial data it is creating more and more user interest. Data capture is faster and cheaper compared to other methods and all the scanned parts are transformed into point-cloud, which can be used repeatedly and for different purposes. Over recent years 3D laser scanning has become a very important method of recording information about objects. The most important advantage is the greater number of spatial points' coordinates that represent the surface of the scanned object, which is obtained over a shorter time interval.

The 3D shape of a physical object is calculated by measuring the length of the laser beam, which is oriented towards the object by the laser scanner (see Fig. 5). There are also 3D scanners that capture the shapes of the objects by using white light rather than lasers. These scanners create patterns of black and white lines on physical objects through which the shape is detected. The obtained model can be treated using various CAD programs (e.g. Geomagic, SolidWorks, Rhino-ceros, etc.).

Three-dimensional scanner ATOS II operates on the principle of triangulation. It consists of the projector and the two digital cameras. The projector projects a structured light (stripes) on the scanned object and then with two cameras (at different angles) the deformation of pattern of light on the object is recorded. Then three-dimensional coordinates of individual points on the object are calculated by the algorithm in the software package (GOM Inspect).

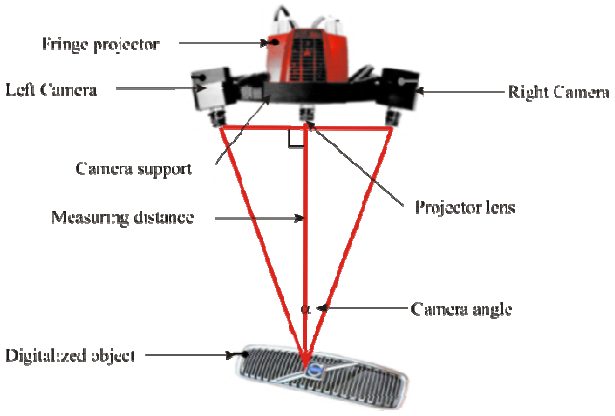

Fig. 5. Principle of 3D scanner.

4. 3D SCANNED DATA PROCESSING

Figure 6 shows the post-processing of the obtained data (scanned area) in the software package GOM Inspect. 1000 points on the surface of the model were randomly measured with the program and through the calculation average roughness R_a of each sample was obtained. Measured surface roughness of the samples made at different laser cladding parameters are shown in Table 2.

The aim of the research is to build a database, which will store all the optimal parameters of the final product and which will give us predicted data on the basis of forecasts by using the artificial methods for every repair with laser cladding of the new piece with the totally new geometry.

This database would help us by choosing a proper filler material, by setting of optimal laser cladding parameters and of course, the resulting surface roughness after laser cladding process. Very good surface quality, which would not require a lot of re-machining (grinding and milling) could be achieved by consideration of all this recommend-data that have been achieved in the previous samples.

The worst surface roughness of graded material is obtained at lower speeds of laser cladding, but in this case due to the thermal influence of the laser, basic material is aggravating in the re-melted zone (a mixture of the basic and filler material). This has a negative impact on the change of microstructure.

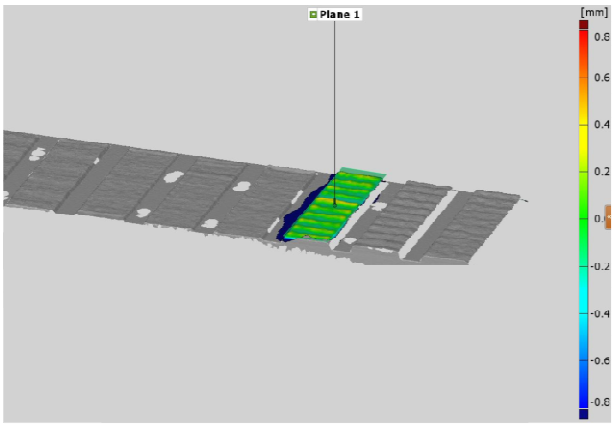

Fig. 6. Data processing in the software package.

Table 2

The resulting surface roughness by different laser cladding parameters

No.	Nozzle speed [%]	Laser power [W]	Average surface roughness [µm]
1	50	400	31.7
2	80		23.5
3	100		14.8
4	50	380	19.3
5	80		17.6
6	100		15.1
7	150	350	13.8
8	130		16.9
9	120		26.2

5. SAMPLE PREPARATION

The commercial AISI 316 stainless steel powder used had a size distribution of between 45 µm and 150 µm. The substrate used was a Cr-Mo steel in annealed condition. On the basis of optical microscopy it was determined that the powder had a substantial level of gas porosity, which has been known to introduce gaseous porosity in the finished SLM product [6]. The powder was embedded in resin for optical observations.

The samples were then EDM cut from the deposited layers and prepared for observations by grinding with SiC paper to P600 and then polishing with 9 µm, 3 µm and 1 µm diamond suspensions. To reveal the microstructure we used etching with saturated picral, and Ralph's reagent. Picral has proven useful since it demanded no special protection of the les noble substrate. The cladded layer was then observed using optical and scanning electron microscopy. The microstructures exhibited cellular and cellular-dendritic morphologies, depending on the cooling rate. The shapes of the pores ranged from small round pores introduced from entrapped gas to hot tearing defects originating from the cooling conditions and process specific porosity. The total fraction of porosity was evaluated matalographicaly from image analysis of optical micrographs of the polished surfaces. Microstructural changes and characteristic defects with varying processing parameters are shown in Fig. 7.

In order to ensure a certain repeatability of the results, three samples were produced using the same processing parameters. We then measured the thickness of the cladded layer, extent of porosity, the fraction of delta ferrite and hardness. The hardness profile was measured along the whole thickness of the cladded layer using adequate spacing between each measurement.

The powder flow-rate was held constant at 0.5 kg/h, and the most efficient tool path was used. The power inputs, tool speeds, contours and hatch parameters were varied, these parameters chosen are summarised in Table 2.

Table 3 shows the key characteristics of the deposited layers.

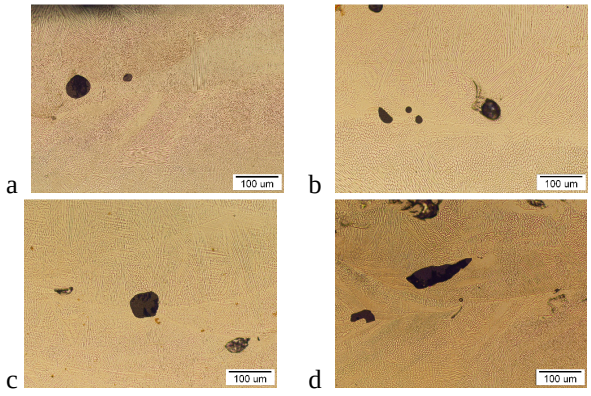

Fig. 7. Microstructural changes and characteristic defects with varying processing parameters: *a* – sample 2, *b* – sample 4, *c* – sample 6, *d* – sample 8 (for all characteristics of each sample see Table 2).

Table 3

Key characteristics of the deposited layer

Sample	Height of deposited layer [mm]	Hardness [HV1]	Fraction of delta ferrite [%]	Fraction of porosity [%]
1	1.05	250	3.6	1.48
2	1.45	270	2	2.78
3	0.86	210	1.75	6.65
4	1.06	265	4.25	1.82
5	1.57	207	2	4.16
6	2.72	245	2	4.07
7	2.21	271	6	0.68
8	1.14	280	5	2.63
9	2.46	254	2.5	24.4

Our microstructural observations (Fig. 8) determined a low density of roundly-shaped pores that could be attributed to gaseous porosity. The observations strongly suggested that the extent of gas porosity was inversely proportional to the introduced energy, and proportional to the feeding speed. This seemed intuitive since the entrapped gas had ample opportunity to escape from a thinner deposited layer and also if the preceding layer were re-melted to a greater extent [7]. This was similar to the re-melting step suggested in [8, 9] but without the apparent loss in productivity. A higher energy input also lowered the cooling rates, which is known to be beneficial for reducing the residual stresses [10], and the extent of porosity in general [11].

The microstructure of the cladded layer consisted of columnar grains oriented according to the heat flow, with a cellular substructure within the grains [12]. The strength correlated according to the sizes of the cells. It is reasonable to assume that the fracture toughness depends predominantly on the sizes of the columnar grains, and not the fine cellular interior. When selecting which microstructural features to monitor, the height of the deposited layer was of obvious significance as a certain thickness would be specified upon application. Hardness values were measured along the normal cross-section. The value given in the table has been averaged from the measurements between the second layer to the top. In all cases the hardness was highest at the fusion layer with the substrate and then became more or less constant towards the top. It is known that a certain volume fraction of delta ferrite acts beneficially on the toughness, as delta ferrite is much efficient in absorbing impurities [10].

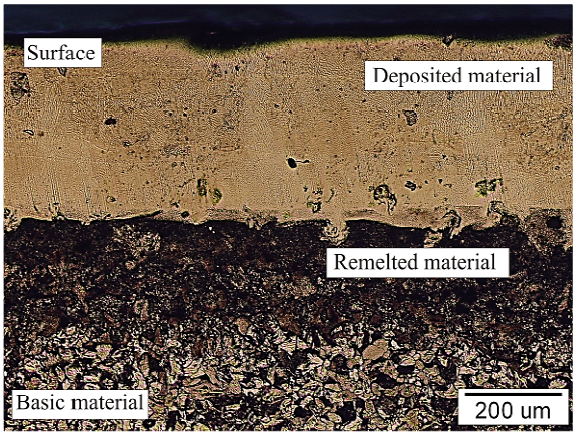

Fig. 8. A sample of laser cladding layers.

Higher scanning speeds conclusively correlated with an increase in the fraction of porosity, without any appreciable correlation with the amount of deposited material. Studies on the compaction of stainless steel powders [9], and finite element modelling [11], generally predict an increase in the latter. However the speeds used in the current study were significantly faster, outlining a suitable processing window. The better overall results were obtained with the slowest scanning speeds used and high energy inputs, thus resulted in thick, almost fully dense deposited layers of relatively high hardness. The lesser extent of porosity in these samples was attributed to the slower cooling rate and a higher fraction of eutectoid ferrite [10]. Both of these also provided strong bonding with the substrates and between adjacent layers. It is worth noting that significant improvements can be achieved by adjusting the laser itself to the specific powder to be melted, this could in future greatly improve the stability of such processes [12].

6. MILLING FUNCTIONALLY-GRADED MATERIAL

The milling of the work-pieces made of graded material was done on a Heller BEA 01 CNC milling machine. Material 42CrMo4 (hardness 23 HRC) was used as the basic material (Fig. 2 and Fig. 3), whilst the mixture of the basic material and deposit material 316L (hardness 65 HRC) was used for creating the graded layer which was 2.5 mm thick.

The cutting parameters used during the experiment were: spindle speed n = 3000 to 4000 rpm, feed rate f = 200 to 1200 mm/min and cutting depth ap = 0.5 mm. Examples of the measured maximum cutting forces *Fx*, *Fy* and *Fz* by milling the graded material are shown in Table 4.

Examples of the measured minimum cutting forces *Fx*, *Fy* and *Fz* by milling the graded material are shown in Table 5 and absolute average cutting forces in Table 6.

The cutting forces were measured using the system shown in Fig. 9. The main parts of the cutting force measuring system are: CNC machine with CNC controller, dynamometer, charge amplifier, data acquisition, software for optimization.

Table 4

Measured maximum forces in *X*, *Y* and *Z* directions by milling of graded material by cutting depth 0.5 mm

Revolutions n [min^{-1}]	Feed f [mm/min]	$F_{x\,max}$ [N]	$F_{y\,max}$ [N]	$F_{z\,max}$ [N]
3000	200	205.40	577.20	344.50
3000	400	302.80	672.60	439.60
3000	800	430.60	800.20	567.50
3500	200	265.70	790.90	459.70
3500	400	360.30	971.70	531.90
3500	800	488.80	1138.80	590.40
3500	1000	463.20	1152.90	626.80
4000	200	429.10	1089.60	509.90
4000	400	606.10	1482.80	590.20
4000	800	849.10	1861.60	657.70
4000	1000	805.50	1824.70	695.50
4000	1200	947.30	2101.60	885.20

Table 5

Measured minimum forces in *X*, *Y* and *Z* directions by milling of graded material by cutting depth 0.5 mm

Revolutions n [min^{-1}]	Feed f [mm/min]	$F_{x\,min}$ [N]	$F_{y\,min}$ [N]	$F_{z\,min}$ [N]
3000	200	–450.90	–1236.40	–288.20
3000	400	–495.70	1381.40	–433.10
3000	800	–740.90	–1626.50	–678.40
3500	200	–31330	–995.90	–284.10
3500	400	–458.10	–1184.80	–351.70
3500	800	–703.30	–1540.90	–442.50
3500	1000	–712.80	–1689.40	–434.20
4000	200	–564.80	–1448.90	–299.20
4000	400	–644.40	–1698.30	–428.90
4000	800	–895.40	–1997.70	–605.80
4000	1000	–844.60	–2122.60	–578.90
4000	1200	–1092.50	–2457.30	–700.20

Table 6

Absolute average cutting forces in *X*, *Y* and *Z* directions by the milling of graded material (revolutions 3000 min^{-1}, feed 200 mm/min and cutting depth 0.5 mm)

Nr.	F_x [N]	F_y [N]	F_z [N]
1	328.15	906.80	316.35
2	399.25	1027.00	436.35
3	585.75	1213.35	622.95
4	289.50	893.40	371.90
5	409.20	1078.25	441.80
6	596.05	1339.85	516.45
7	496.95	1269.25	404.55
8	625.25	1590.55	509.55
9	872.25	1929.65	631.75

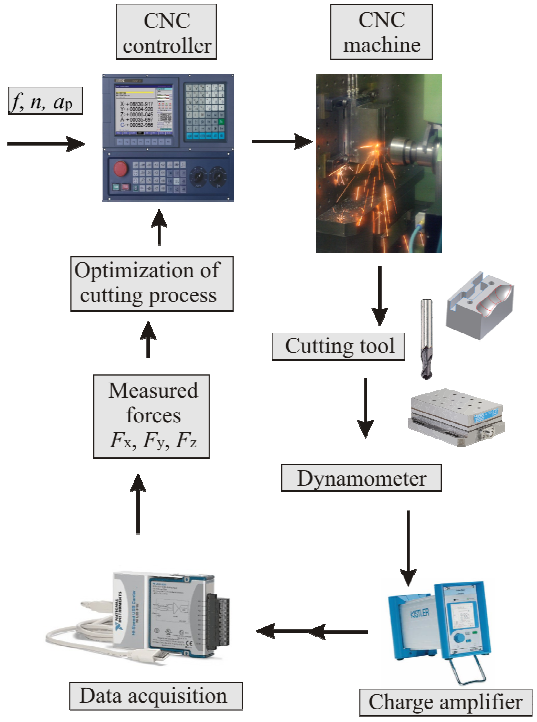

Fig. 9. Cutting force measuring system.

7. PREDICTION OF CUTTING FORCES BY USING ANN

In our experiment, the more commonly used technique of the feed-forward back-propagation neural network was adapted for predicting the cutting forces during the milling operation. It consisted of an input layer (where the inputs of the problem were received), hidden layers (where the relationships between the inputs and outputs were determined) and an output layer (which emitted the output of the problem).

The input parameters for the neural network were depth of cut (a_p) and feed-rate (f). The input parameters influenced most on the sizes of the cutting forces in all three directions of the coordinated system, which were the output parameters of ANN.

Cutting forces when milling the layers of graded material were measured in both the positive and negative directions. The measured negative values of the cutting forces only had opposite orientation within the space of the relatively assumed coordinate system. It was necessary to take both data for each direction of the coordinate system (*X*, *Y* and *Z*).

The best results having smaller errors of predicted cutting forces by milling the graded material (layer) were achieved by the neural network with 2 hidden layers. The input components (input layer) of the neural network were depth of cut *ap* and milling feed f and the output components were cutting forces *Fx*, *Fy* and *Fz*. Between the input and the output of the neural network were 2 hidden layers with 6 and 3 neurons.

Table 7 presents predicted cutting forces in *X*, *Y* and *Z* directions by milling layer of functionally-graded material by the usage of ANN.

The training results of ANN for predicting cutting forces in the main directions of the coordinate system are shown in Table 3. The maximum learning error of the neural network was less than 10 %, which is acceptable for our further work and for predicting new results. Error in % between measured and predicted cutting forces by ANN usage are shown in Table 8.

Table 7

Predicted cutting forces in *X*, *Y* and *Z* directions by milling layer of functionally-graded material by the usage of ANN

Nr.	Predicted forces		
	F_x [N]	F_y [N]	F_z [N]
1	351.65	819.29	339.73
2	377.37	1044.05	475.36
3	594.01	1260.55	673.16
4	309.48	961.48	340.47
5	416.07	1101.86	476.92
6	651.36	1243.78	564.79
7	471.85	1353.27	432.30
8	680.83	1714.77	560.00
9	874.87	1892.99	644.64

Table 8

Error in % between measured and predicted cutting forces by ANN usage

Nr.	Error F_x [%]	Error F_y [%]	Error F_z [%]
1	7.16	–9.65	7.39
2	–5.48	1.66	8.94
3	1.41	3.89	8.06
4	6.90	7.62	–8.45
5	1.68	2.19	7.95
6	9.28	–7.17	9.36
7	–5.05	6.62	6.86
8	8.89	7.81	9.90
9	0.30	–1.90	2.04

8. CONCLUSIONS

This paper only presents those first obtained results that would serve us for further database construction. The further idea was that all the influential factors would be in the pre-built database that would be obtained on the bases of the experiments. In any case, the test would continue in the direction of optimising the quality of the resulting graded material and surface roughness in the direction of minimising the re-machining processes (milling or grinding) and for minimising additional costs. The first results of milling very hard material such as graded material showed us that the machining of such materials is possible.

The idea is to establish a direct connection between laser cladding, properties of layers of graded material (roughness) and re-machining of it with milling, where the cutting forces were measured, was fully realized.

The first results of the values of several parameters were satisfactorily predicted as a model for the prediction by using neural networks.

The results of the prediction of cutting forces in post-processing are favourable. The errors between predicted and measured cutting forces by milling at different conditions (cutting speed, feed-rate, cutting depth) of graded material (layers) were less than 10 %. Next step is to find better prediction model, which will give us predicted results with smaller error. To achieve stated goal, also genetic algorithms and new algorithms of neural networks will be used. This is a very reliable prediction for the planned cutting force that will allow us to operate the machine within safer areas.

In the future we would like to upgrade our database, add some new basic and deposited materials, find more combinations of graded material and as a main priority to find the best parameters for the laser-cladding machine, which would provide very good surface roughness and no additional re-machining would be required. For such a prediction we will continue using neural networks but with the idea of also including genetic algorithms.

REFERENCES

[1] E. Capello, D. Colombo, B. Previtali, *Repairing of Sintered Tools Using Laser Cladding by Wire*, Journal of Materials Processing Technology, Vol. 164–165, 2005, pp. 990–1000.

[2] A. Joshi, A. Patnaik, B. Gangil, S. Kumar, *Laser Assisted Rapid Manufacturing Technique for the Manufacturing of Functionally Graded Materials*, SCES - Student Conference on Engineering and Systems, 2012, pp. 1–3.

[3] A.P. Tadamalle, Y.P. Reddy, E. Ramjee, *Influence of Laser Welding Process Parameters on Weld Pool Geometry Duty Cycle*, Advances in Production Engineering & Management, Vol. 1, 2013, pp. 52–60.

[4] M. Brandt, S. Sun, N. Alam, P. Bendeich, A. Bishop, *Laser Cladding Repair of Turbine Blades in Power Plants*, International Heat Treatment & Surface Engineering, Vol. 3, No. 3, 2009, pp. 105–114.

[5] Y. Yakovlev, P. Bertrand, I. Smurov, *Laser Cladding of Wear Resistant Metal Matrix Composite Coatings*, Thin Solid Films, Vol. 453-454, 2004, pp. 133–138.

[6] H.-A. Bahr, H. Balke, T. Fett, I. Hofinger, G. Kirchhoff, D. Munz, A. Neubrand, A.S. Semenov, H.-J. Weiss, Y.Y. Yang, *Cracks in Functionally Graded Materials*, Materials science & Engineering, Vol. 362, No. 1–2, 2003, pp. 2–16.

[7] S. Lijung, J. Mazumder, *Feedback Control of Melt Pool Temperature During Laser Cladding Process*, Control system technology, Vol. 19, No. 6, 2011, pp. 1349–1356.

[8] M. Babic, J. Balic, M. Milfelner, I. Belic, P. Kokol, M. Zorman, P. Panjan, *Robot Laser Hardening and the Problem of Overlapping Laser Beam*, Advances in Production Engineering & Management, Vol. 8, No. 1, 2013, pp. 25–32.

[9] M. Chandrasekaran, D. Devarasiddappa, *Artificial Neural Network Modeling for Surface Roughness Prediction in Cylindrical Grinding of Al-SiCp Metal Matrix Composites and ANOVA Analysis*, Advances in Production Engineering & Management, Vol. 9, No. 2, 2014, pp. 59–70.

[10 L. Ruidi, S. Yusheng, W. Li, L. Jinhui, W. Zhigang, *The key metallurgical features of selective laser melting of stainless steel*, Powder Metallurgy and Metal Ceramics, Vol. 50, No 3–4, 2011, pp. 141–150.

[11] X. Peng, L. Cheng Xin, Z. Chao Yu, Y. Xin Peng, *Wear and corrosion resistance of laser cladding AISI 304 stainless steel/Al2O3*, Composite coatings, Vol. 238, 2014, pp. 9–14.

[12] J.W. Elmer, S.M. Allen, T.W. Eagar, 1989, *Microstructural development during solidify-cation of stainless steel alloys*, Metallurgical Transactions A, Vol. 20, No. 10, 1989, pp. 2117–2131.